# Collider Test of Type III Seesaw Model

Guiyu Huang

University of Wisconsin - Madison

Pheno 2008

work in progress with

A.Arhrib, B.Bajc, D.K.Ghosh, T.Han, I.Puljak, G.Senjanović

**For similar study of Type II model see**

arXiv:0803.3450 and talk by Tong Li.

# Outline

# Neutrino Mass

Neutrino oscillation experiments show non-zero neutrino mass differences $\Delta m^2_{sol}$ and $\Delta m^2_{atm}$, thus implying at least two massive neutrinos.

## Seesaw Mechanism

Neutrino mass generated by

$$\mathcal{L}_{eff} = y_{eff} \frac{LLHH}{M}$$

where $M \gg M_W$.

In general, the small neutrino masses can be explained by large $M$, or small Yukawa, or both.

# Seesaw Classification

Depending on the nature of the heavy degrees of freedom, seesaw models can be classified as

- I. SM femionic singlets,
- II. SU(2) bosonic triplet (Y=2),
- III. SU(2) fermionic triplet (Y=0),
- and... combination of I and III. (Natural from $24_F$ of SU(5) GUT)

# Type III Seesaw

$SU_L(2)$ lepton triplet $T = (T^+, T^0, T^-)$ (1,3,0), and lepton singlet $S$. The Majorana mass and the Yukawa interactions are

$$\begin{aligned} - & \; M_T(T^+T^- + T^0T^0/2) - M_S(SS/2) \\ + & \; y_T^i H^T i\sigma_2 T L_i + y_S^i H^T i\sigma_2 S L_i + h.c. \end{aligned}$$

These lead to the Majorana mass for the light neutrinos

$$M_{ij} \approx \frac{v^2}{2}\left(\frac{y_T^i y_T^j}{m_T} + \frac{y_S^i y_S^j}{m_S}\right),$$

From flavor to mass eigenstates, mixings occur such as

$$T^0 \to T^0 - \epsilon_T^i \nu_i, \qquad \epsilon_X^i \equiv \frac{y_X^i v}{\sqrt{2} m_X}$$

Heavy scalar. TeV scale triplet.

# Production Channels

Lepton pair production in hadronic collisions is dominantly via the Drell-Yan mechanism,

$$q\bar{q}' \to W^{*\pm} \to T^{\pm}T^{0}, \quad q\bar{q}' \to W^{*\pm} \to T^{0}\ell^{\pm},$$
$$q\bar{q} \to \gamma^{*}, Z \to T^{+}T^{-}, \quad q\bar{q} \to Z^{*} \to T^{\pm}\ell^{\mp}.$$

$$\lambda^2 = \begin{cases} 1 & \text{for } TT \\ \sum_i |y_i|^2 & \text{for } T\ell. \end{cases}$$

# Cross sections at LHC

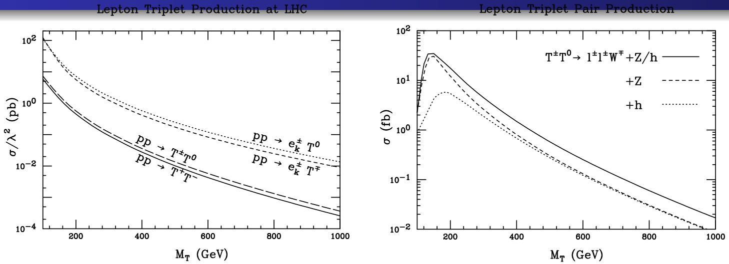


(a) (b)

Figure: Total cross section for $Z'$ production versus its mass, (a) with the coupling constant squared ($\lambda^2$) factored out (for states in the KK eigenbasis), and (b) with the absolute normalization for the couplings (for states in the mass eigenbasis).

# Total Widths

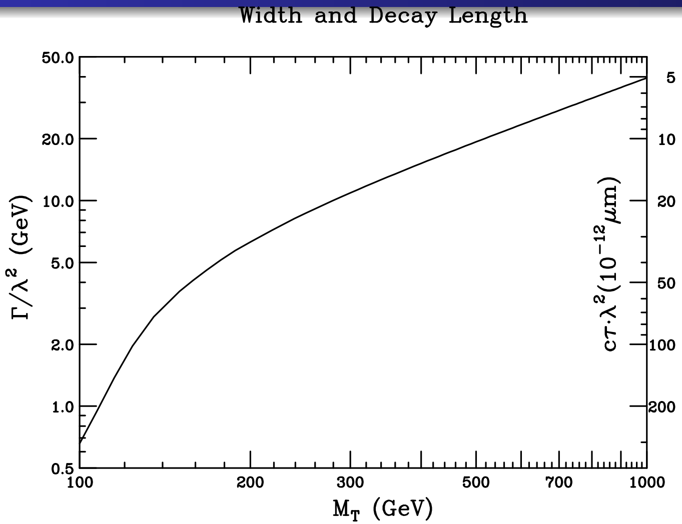


Figure: The total width of $T$ as a function of its mass.

# Branchings

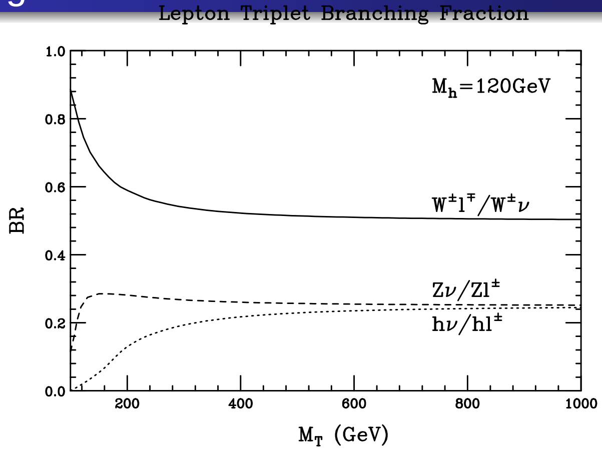


Figure: The branching ratios of $T$ into the various modes as a function of its mass.

# Decay Modes of a $TT$ Pair

The possible combinations of decay channels of pair-produced $T$'s.

| | $T^- \to \nu W^-$ | $T^- \to \ell^- Z$ | $T^- \to \ell^- h$ |
|---|---|---|---|
| $T^0 \to \nu h$ | $\nu\nu W^- h$ | $\nu\ell^- Zh$ | $\nu\ell^- hh$ |
| $T^0 \to \nu Z$ | $\nu\nu W^- Z$ | $\nu\ell^- ZZ$ | $\nu\ell^- Zh$ |
| $T^0 \to \ell^- W^+$ | $\nu\ell^- W^- W^+$ | $\ell^-\ell^- W^+ Z$ | $\ell^-\ell^- W^+ h$ |
| $T^0 \to \ell^+ W^-$ | $\nu\ell^+ W^- W^-$ | $\ell^+\ell^- W^- Z$ | $\ell^+\ell^- W^- h$ |
| $T^+ \to \nu W^+$ | $\nu\nu W^- W^+$ | $\nu\ell^- W^+ Z$ | $\nu\ell^- W^+ h$ |
| $T^+ \to \ell^+ Z$ | $\nu\ell^+ W^- Z$ | $\ell^+\ell^- ZZ$ | $\ell^+\ell^- Zh$ |
| $T^+ \to \ell^+ h$ | $\nu\ell^+ W^- h$ | $\ell^+\ell^- Zh$ | $\ell^+\ell^- hh$ |

Table: Triplet pair decay channels.

# Background

Dominant background is expected from $t\bar{t}W$ events.

$$t\bar{t}W^{\pm} \to bW^{+}\bar{b}W^{-}W^{\pm} \to \ell^{\pm}\ell^{\pm}b\bar{b}jj\nu\nu$$

Other backgrounds include $WWWW$ and $WWWZ$ and generic $WWWjj$ . $WWZZ$ events do not yield same-sign leptons.
Jets faking leptons should also be considered.

# Parametrizing the Type III Yukawas

In normal hierarchy (NH) i.e. $m_1^\nu = 0$,

$$\frac{vy_T^{i*}}{\sqrt{2}} = i\sqrt{m_T}\left(U_{i2}\sqrt{m_2^\nu}\cos z \pm U_{i3}\sqrt{m_3^\nu}\sin z\right)$$

$$\frac{vy_S^{i*}}{\sqrt{2}} = -i\sqrt{m_S}\left(U_{i2}\sqrt{m_2^\nu}\sin z \mp U_{i3}\sqrt{m_3^\nu}\cos z\right)$$

In inverted hierarchy (IH) i.e. $m_3^\nu = 0$,

$$\frac{vy_T^{i*}}{\sqrt{2}} = i\sqrt{m_T}\left(U_{i1}\sqrt{m_1^\nu}\cos z \pm U_{i2}\sqrt{m_2^\nu}\sin z\right)$$

$$\frac{vy_S^{i*}}{\sqrt{2}} = -i\sqrt{m_S}\left(U_{i1}\sqrt{m_1^\nu}\sin z \mp U_{i2}\sqrt{m_2^\nu}\cos z\right)$$

where $z$ is a complex number.

# PMNS matrix

The PMNS neutrino mixing matrix

$$
\begin{aligned}
U &= \begin{pmatrix} c_{12}c_{13} & c_{13}s_{12} & e^{-\mathrm{i}\delta}s_{13} \\ -c_{12}s_{13}s_{23}e^{\mathrm{i}\delta} - c_{23}s_{12} & c_{12}c_{23} - e^{\mathrm{i}\delta}s_{12}s_{13}s_{23} & c_{13}s_{23} \\ s_{12}s_{23} - e^{\mathrm{i}\delta}c_{12}c_{23}s_{13} & -c_{23}s_{12}s_{13}e^{\mathrm{i}\delta} - c_{12}s_{23} & c_{13}c_{23} \end{pmatrix} \\
&\times \quad \mathrm{diag}(e^{i\Phi_1/2}, 1, e^{i\Phi_2/2})
\end{aligned}
$$

# Neutrino Data Fitting

| Parameter | Best fit | $2\sigma$ | $3\sigma$ |
|---|---|---|---|
| $\Delta m^2_{21}$ $[10^{-5}\mathrm{eV}^2]$ | 7.6 | 7.3–8.1 | 7.1–8.3 |
| $\lvert\Delta m^2_{31}\rvert$ $[10^{-3}\mathrm{eV}^2]$ | 2.4 | 2.1–2.7 | 2.0–2.8 |
| $\sin^2\theta_{12}$ | 0.32 | 0.28–0.37 | 0.26–0.40 |
| $\sin^2\theta_{23}$ | 0.50 | 0.38–0.63 | 0.34–0.67 |
| $\sin^2\theta_{13}$ | 0.007 | $\leq 0.033$ | $\leq 0.050$ |

Table: Best-fit values, $2\sigma$ and $3\sigma$ intervals (1 d.o.f.) for the three–flavour neutrino oscillation parameters from global data including solar, atmospheric, reactor (KamLAND and CHOOZ) and accelerator (K2K and MINOS) experiments.

Parametrically, $y_X^i$ grows exponentially with $\mathrm{Im}(z)$. Not bound from above.
Constrained by low energy rare processes such as $\mu \to e\gamma$.

$$|y| \leq 10^{-5}, \quad \text{i.e.} \quad |\mathrm{Im}(z)| \leq 5 - 6$$

The dimensionless parameter $a_X$ is defined as,

$$a_X^i \equiv \left| y_X^i \right| \sqrt{\frac{v}{2m_X}}$$

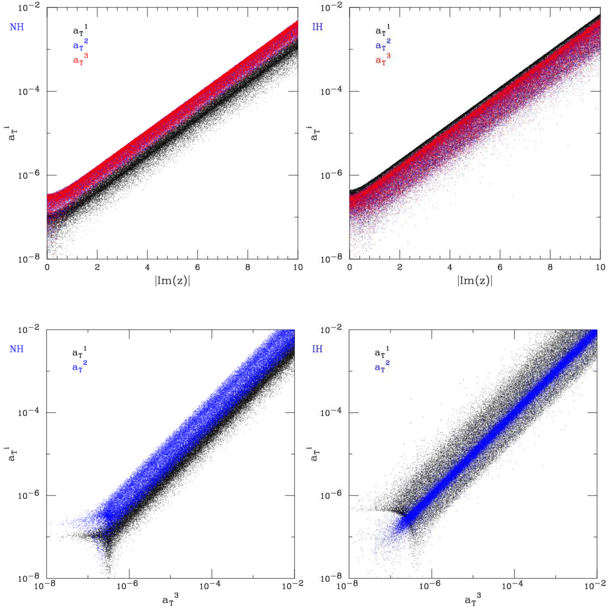
NH
IH
$a_T^1$
$a_T^2$
$a_T^3$
$a_T^i$
|Im(z)|
$a_T^3$
$10^{-2}$
$10^{-4}$
$10^{-6}$
$10^{-8}$
0
2
4
6
8
10

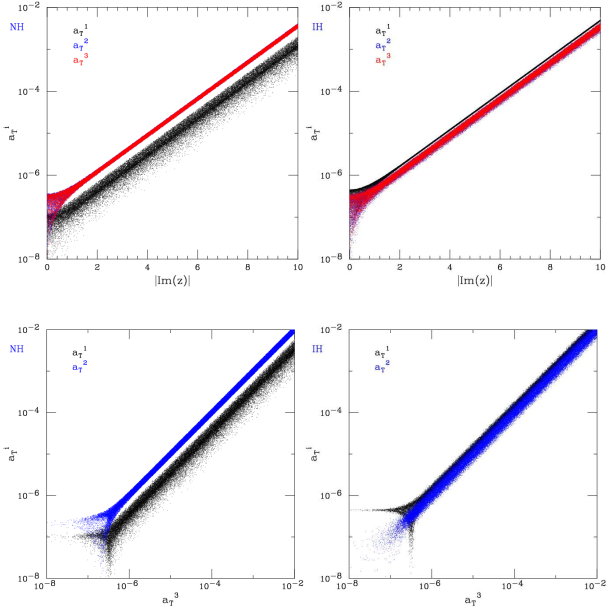
NH
IH
$a_T^1$
$a_T^2$
$a_T^3$
$a_T^i$
|Im(z)|
$a_T^3$
$10^{-2}$
$10^{-4}$
$10^{-6}$
$10^{-8}$
0 2 4 6 8 10

# Normalized Branching

The normalized branching is defined as

$$\frac{\mathrm{BR}(Ve_i)}{\mathrm{BR}(Ve)} \equiv \frac{\mathrm{BR}(Ve_i)}{\Sigma_i \mathrm{BR}(Ve_i)}$$

$\mathrm{BR}(Ve)$ varies with the mass of the triplet. For sufficiently large $m_T$, $\mathrm{BR}(Ve) = 1/2, 1/4, 1/4$ for $V = W, Z, h$.

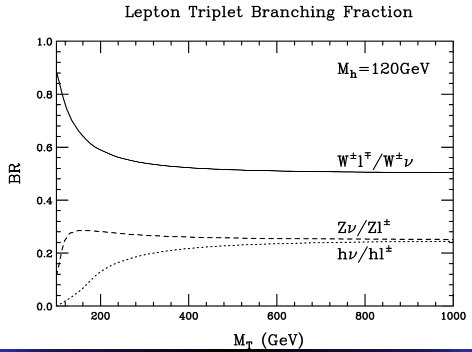

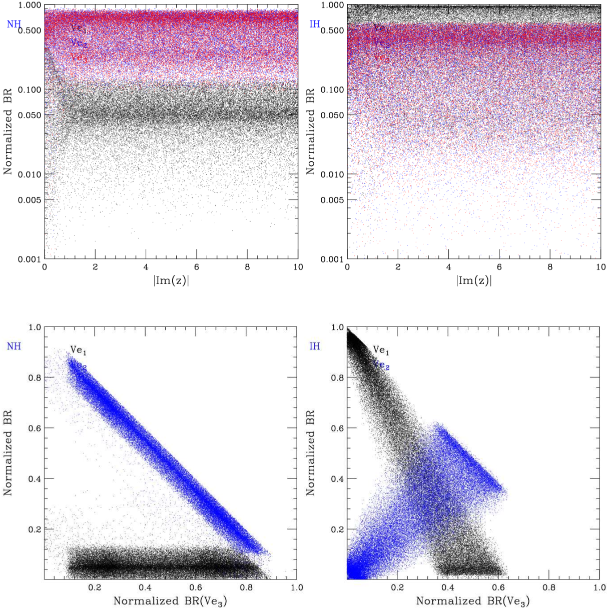
NH
Ve1
Ve2
Ve3
Normalized BR
|Im(z)|
IH
Ve1
Ve2
Ve3
Normalized BR
|Im(z)|
NH
Ve1
Normalized BR
Normalized BR(Ve3)
IH
Ve1
Ve2
Normalized BR
Normalized BR(Ve3)

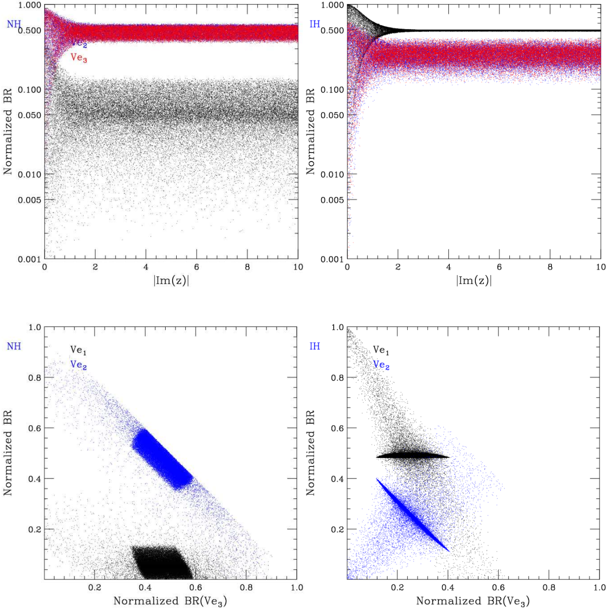
NH
Ve2
Ve3
Normalized BR
|Im(z)|
IH
Ve1
Ve2
Normalized BR(Ve3)

In most parameter space of NH, the normalized branchings for $V\mu$ and $V\tau$ are between 0.1 to 0.9. They sum up to more than 0.85 and the normalized $Ve$ branching is less than 0.15 in most regions . So,

$$\mathrm{BR}(V\mu, V\tau) \gg \mathrm{BR}(Ve),$$

Therefore for pair produced $TT$, we can establish a hierachical order among the branchings of their decay combinations:

$$\mu\mu, \mu\tau, \tau\tau \gg e\mu, e\tau \gg ee. \quad (1)$$

For the IH it is more complicated. A quasi-seperation can also be established for IH if Majorana phases are fixed.

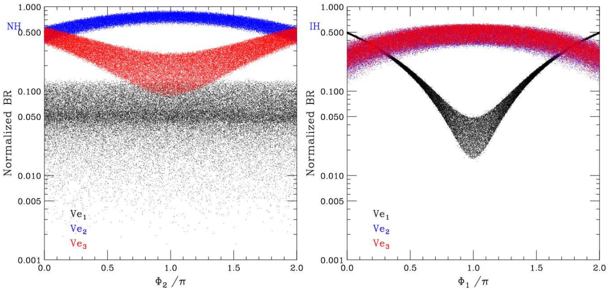


Figure: Normalized branching vs Majorana phases for NH (left) and IH (right). $\mathrm{Im}(z) \geq 2$, $s_{13}^2 \leq 0.033$ and $\Phi_{1,2} \in [0, 2\pi]$. The NH (IH) has no dependence on $\Phi_1(\Phi_2)$.

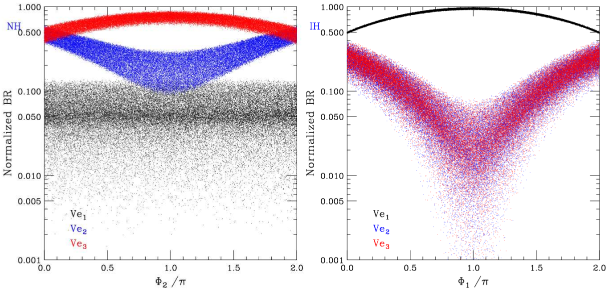


Figure: Normalized branching vs Majorana phases for NH (left) and IH (right). $\mathrm{Im}(z) \leq -2$, $s_{13}^2 \leq 0.033$ and $\Phi_{1,2} \in [0, 2\pi]$. The NH (IH) has no dependence on $\Phi_1(\Phi_2)$.

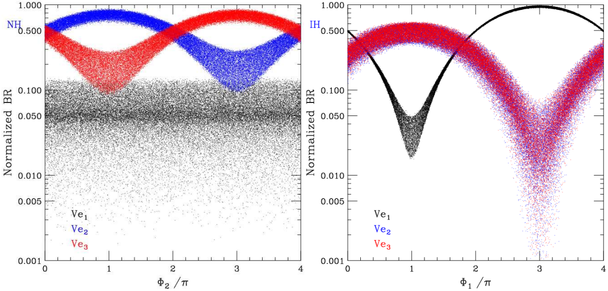


Figure: Normalized branching vs Majorana phases for NH (left) and IH (right). $\mathrm{Im}(z) \geq 2$ and $\Phi_{1,2} \in [0, 4\pi]$.

As $\Phi_{1,2}$ only appear as $\Phi_{1,2}/2$, the appropriate periodicity range is therefore $\Phi_{1,2} \in [0, 4\pi]$.
On the other hand, we notice that $y_T^i \leftrightarrow \pm y_T^i$ (plus sign for NH and minus for IH) under the symmetry transformation $(\Phi_i \leftrightarrow \Phi_i + 2\pi, z \leftrightarrow -z)$. Thus $|y_T^i|$ and $\mathrm{BR}(Ve_i)$ are invariant under said symmetry.

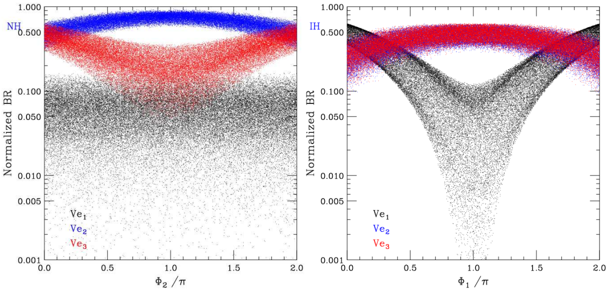


Figure: Normalized branching vs Majorana phases for NH (left) and IH (right). $\mathrm{Im}(z) = 1$, and $\Phi_{1,2} \in [0, 2\pi]$. The NH (IH) has no dependence on $\Phi_1(\Phi_2)$.

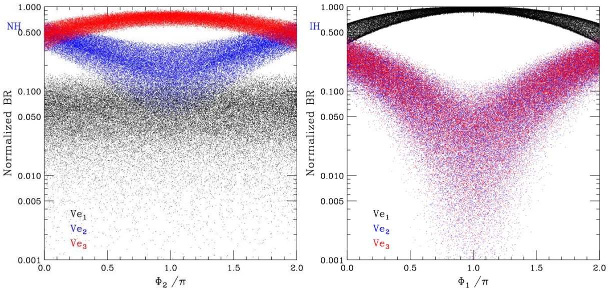


Figure: Normalized branching vs Majorana phases for NH (left) and IH (right). $\mathrm{Im}(z) = 1$, and $\Phi_{1,2} \in [0, 2\pi]$. The NH (IH) has no dependence on $\Phi_1(\Phi_2)$.

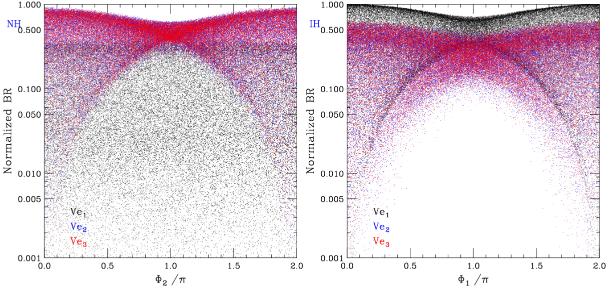


Figure: Normalized branching vs Majorana phases for NH (left) and IH (right). $\mathrm{Im}(z) = 0$, and $\Phi_{1,2} \in [0, 2\pi]$. The NH (IH) has no dependence on $\Phi_1(\Phi_2)$.

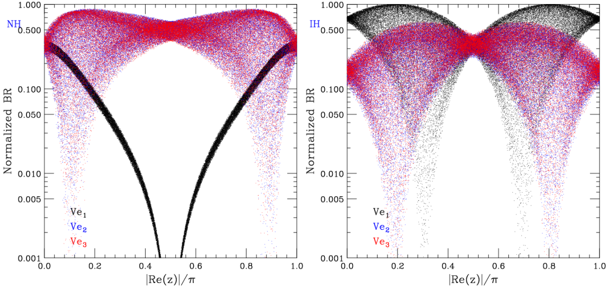


Figure: Normalized branching vs $|\mathrm{Re}(z)|$ for NH (left) and IH (right). $\mathrm{Im}(z) = 0$, and $\Phi_{1,2} \in [0, 2\pi]$.